

Title: Evidence for multiple bulbar and higher brain circuits processing sensory inputs from the respiratory system in humans

Running Title: Respiratory sensory pathways in humans

Authors: Michael J. Farrell ^{1,2}, Tara G. Bautista ^{1,3}, Emma Liang ², Damian Azzollini ², Gary F. Egan ^{2,4,5}, Stuart B. Mazzone ³

1. Departmental of Medical Imaging and Radiation Sciences, Monash University, Clayton VIC, Australia 3800
2. Monash Biomedical Imaging, Monash University, Clayton VIC, Australia 3800
3. Department of Anatomy and Neuroscience, University of Melbourne, Parkville VIC, Australia 3010
4. School of Psychological Sciences, Monash University, Clayton VIC, Australia 3800
5. ARC Centre of Excellence for Integrative Brain Function, Monash University, Clayton VIC, Australia 3800

Corresponding author:

Stuart B Mazzone Email: stuart.mazzone@unimelb.edu.au

Number of pages: 39

Number of figures: 6 tables: 3

Number of words for abstract: 251 introduction: 577 discussion: 2008

This is the author manuscript accepted for publication and has undergone full peer review but has not been through the copyediting, typesetting, pagination and proofreading process, which may lead to differences between this version and the [Version of Record](#). Please cite this article as [doi: 10.1113/jphysiol.2013.14379](https://doi.org/10.1113/jphysiol.2013.14379).

This article is protected by copyright. All rights reserved.

Additional information

Conflict of interest statement

SBM reports receiving consultancy fees from Merck Sharpe and Dohme and Nerre Therapeutics for services unrelated to the work reported in this manuscript. All other authors declare no conflict of interest.

Author contributions

TGB, EL and DA conducted and analysed the experiments. SM and MF conceived and designed experiments and wrote the manuscript. GFE contributed to the design of data analysis. All authors contributed to interpretation of data and editing of the manuscript. Experiments were conducted in the research laboratories of Professor Mazzone at the University of Melbourne and Associate Professor Farrell at Monash Biomedical Imaging. All authors have approved the final version of the manuscript and agree to be accountable for all aspects of the work presented in the manuscript. All persons designated as authors qualify for authorship and all those that qualify have been listed as authors.

Funding

This research was supported by grants to SBM and MJF from the National Health and Medical Research Council (NHMRC) of Australia [1078943]. TGB held a Research Fellowship Grant from The Garnett Passe and Rodney Williams Memorial Foundation of Australia.

Acknowledgements

The authors would like to gratefully acknowledge the support of the Garnett Passe and Rodney Williams Memorial Foundation of Australia.

Key words

Vagal sensory; Cough; Brain imaging; Purinergic; Brainstem

Edited by: Harold Schultz & Weifang Rong

Data availability

All data supporting the results presented in the manuscript are included in the manuscript figures as n were ≤ 30 . The data that support the findings of this study are available on request from the corresponding author.

This article is protected by copyright. All rights reserved.

Key points summary

Author Manuscript

- Unpleasant respiratory sensations contribute to morbidity in pulmonary disease. In rodents, these sensations are processed by nodose and jugular vagal sensory neurons, two distinct cell populations that differentially project to the airways and brainstem.
- Whether similar differences exist in bronchopulmonary sensory pathways in humans is unknown.
- We use fMRI during inhalation of capsaicin and ATP, showing that airway nodose pathways project centrally to the nucleus of the solitary tract while jugular pathways input into the trigeminal brainstem nuclei.
- We also show differences between the efficacy of nodose and jugular stimuli to evoke cough and activity in motor control regions of the brain.
- Our data argue that humans have two distinct vagal sensory neural systems governing airway sensations and this may have implications for the development of new antitussive therapies.

Abstract

In rodents, nodose vagal sensory neurons preferentially innervate the distal airways and terminate centrally in the nucleus of the solitary tract. By contrast, jugular vagal sensory neurons preferentially innervate the proximal airways and terminate in the paratrigeminal nucleus in the dorsolateral medulla. This differential organization suggests distinct roles for nodose and jugular pathways in respiratory sensory processing. However, it is unknown whether bronchopulmonary afferent pathways are similarly arranged in humans. We set out to investigate this using high resolution brainstem and whole brain functional magnetic resonance imaging in healthy human participants while inhaling stimuli known to differentially activate nodose and jugular pathways. Inhalation of capsaicin or adenosine triphosphate (ATP) evoked respiratory sensations described as an urge-to-cough, although ATP was significantly less effective compared to capsaicin at evoking the motor act of coughing. The nodose and jugular neuron stimulant capsaicin increased BOLD signals extending across the dorsomedial and dorsolateral medulla, encompassing regions containing both the nucleus of the solitary tract and the paratrigeminal nucleus. By contrast, at perceptually comparable stimulus intensities, the nodose-selective stimulant ATP resulted in BOLD signal intensity changes that were confined to the area of the nucleus of the solitary tract. During whole brain imaging, capsaicin demonstrated a wider distributed network of activity compared to ATP, with significantly increased activity in regions involved with motor control functions. These data argue that functional and neuroanatomical differences in bronchopulmonary nodose and jugular sensory pathway organization are conserved in humans and that this has implications for understanding the neurobiological mechanisms underpinning cough.

Michael John Farrell investigates regional brain responses in humans associated with the maintenance of the internal state. His research has used neuroimaging techniques including functional magnetic resonance imaging (fMRI), perfusion-related fMRI and positron emission tomography to investigate brain responses in humans associated with interoceptive sensations (pain, urge-to-cough, thirst, temperature sensation), regulatory behaviours (drinking water, coughing and cough suppression), and autonomic responses (thermoregulatory-related vasomotor and sudomotor responses).

Introduction

The respiratory mucosa is innervated by sensory nerve fibres derived principally from vagal origins (Mazzone & Udem, 2016). These sensory fibres are responsible for monitoring the local bronchopulmonary environment, and when activated they drive reflex and behavioural changes to breathing and autonomic outflow that serve to optimize gas exchange and protect the airways and lungs from exogenous and endogenous irritants. Accompanying these sensory-evoked respiratory motor events are perceivable sensations that provide an awareness of the operations of the respiratory system (Davenport, 2009; Ando *et al.*, 2014). For example, the presence of chemical stimuli that activate vagal sensory nerve terminals in the respiratory tract (such as inhaled smoke or locally produced inflammatory mediators) is often perceived as an uncomfortable airway irritation, particularly in the proximal airways, that leads to an overwhelming desire (or urge) to cough (Mazzone *et al.*, 2007a; Davenport, 2009; Ando *et al.*, 2014). Indeed, the urge-to-cough is a respiratory sensory experience reflective of the irritant inputs from the airways and shares many neurophysiological attributes to pain, experienced during noxious stimulation of somatic tissues (Driessen *et al.*, 2016). In pulmonary diseases, the urge-to-cough is a particularly difficult symptom to alleviate and can be an insatiable sensation that contributes substantially to patient morbidity (Hilton *et al.*, 2015). Therefore, understanding the neural substrates involved in respiratory sensory processing and the urge-to-cough is of clinical interest.

Vagal bronchopulmonary sensory neurons arise from two embryologically-distinct sensory neuron lineages (Baker, 2005; D'Autreaux *et al.*, 2011). Neurons of the jugular vagal sensory ganglia are derived from the neural crest whereas the more extensively studied nodose ganglia sensory neurons are derived from the epibranchial placodes. Consequently, jugular and nodose neurons display important functional and neuroanatomical differences. All airway projecting jugular neurons fit the description of chemically-sensitive nociceptors, and are characteristically responsive to the transient receptor potential vanilloid 1 (TRPV1) receptor ligand capsaicin, whereas separate capsaicin-sensitive nociceptor and capsaicin-insensitive mechanosensory neurons comprise the nodose ganglia (reviewed in (Mazzone & Udem, 2016)). Many jugular nociceptors express the neuropeptides substance P and calcitonin gene-related peptide, and are unresponsive to adenosine triphosphate (ATP, and related purinergic ligands), 5-hydroxytryptamine (5-HT) and adenosine (Nassenstein *et al.*, 2010; Chou *et al.*, 2018). By contrast, nodose nociceptors generally do not express neuropeptides, but are responsive to ATP, 5-HT and adenosine (Nassenstein *et al.*, 2010; Chou *et al.*, 2018). Indeed, jugular ganglia neurons may be considered somatic in their representation as they contribute to the sensory innervation of tissues of the head and neck,

including the larynx and large airways, whereas nodose neurons are stereotypically recognised as vagal visceral afferents (D'Autreaux *et al.*, 2011).

We previously reported in rodents that jugular neurons, including those projecting to the airway mucosa, terminate in and around the paratrigeminal nucleus (Pa5) in the caudal medulla, rather than the nucleus of the solitary tract (NTS) where most nodose neurons project (Driessen *et al.*, 2015; McGovern *et al.*, 2015a; McGovern *et al.*, 2015b). Furthermore, the airway sensory circuits arising from the Pa5 are also distinct to those from the NTS (McGovern *et al.*, 2015b), suggesting the existence of multiple airway afferent processing pathways in the rodent brain. However, whether there exists a comparable neuroanatomical arrangement for respiratory sensory processing in the human brain remains unknown. Therefore, in the present study we set out to use functional brain imaging paradigms during inhaled challenges with capsaicin and ATP to investigate whether distinct 'jugular-like' and 'nodose-like' respiratory sensory neural circuits could be deciphered in the human brainstem and higher brain.

Materials and Methods

Ethical Approval

The study and procedures were approved by the Monash University Human Research Ethics Committee (project number 6424) and conform to the standards set by the Declaration of Helsinki (last modified in 2013), except for registration in a database.

Participants

Twenty-two adults gave written, informed consent to participate in the study. Prior to inclusion, all subjects were screened via telephone interview to exclude conditions that could potentially alter cough sensitivity, including chronic respiratory or neurological disease or acute respiratory infection. All subjects were non-smokers, and were not taking any medications likely to influence cough sensitivity or functional magnetic resonance imaging (fMRI) blood oxygen-level dependent (BOLD) responses at the time of testing. One participant withdrew from the study due to claustrophobia associated with scanning, and a second participant was excluded because they did not experience an urge-to-cough sensation during inhalation of ATP. A total of 20 participants (12 female; mean age = 24.4 ± 8.5 years) complied with the protocol and were included in the final analyses.

Inhaled Substances

Participants inhaled three types of nebulised substances during the experiment. Normal saline (0.9% NaCl) was used as a control substance because this stimulus does not evoke coughing or a perceptible urge-to-cough. Doubling concentrations of capsaicin (0.25 μM to 125 μM) or ATP (0.45 mM to 232.5 mM) were prepared as previously described (Mazzone *et al.*, 2007a; Mazzone *et al.*, 2011; Fowles *et al.*, 2017; Morice *et al.*, 2019). Jet nebulisers (RapidFlo; Allersearch, Scoresby, Victoria, Australia) were used to generate vapour ($\sim 2\text{-}3\mu\text{m}$ particle size) for inhalation by participants via a face mask. An air compressor (Liberty Healthcare, Ringwood, Victoria, Australia) delivered air at a flow rate of $\sim 5\text{ L min}^{-1}$ to the nebuliser bowl during a preliminary psychophysical session. During the acquisition of functional brain images, compressed medical air (5 L min^{-1}) was used and a series of parallel shut-off valves directed the air to one of the three nebulisers (containing capsaicin, ATP or saline), or to a vent for passive exhaust during non-stimulus periods. Each nebuliser was connected in parallel to the face mask via independent tubing, preventing direct mixing of test reagents.

Experimental Design

Psychophysical Session – Determination of Sensitivity to inhalations of capsaicin and ATP

Participants undertook single, tidal breaths of successively higher concentrations of capsaicin solutions beginning with the lowest level of 0.25 μM , and an inter-breath interval of at least one minute. Audible coughs were counted in the 30-second period following each breath, after which participants were asked to provide a rating of the level of urge-to-cough experienced during the inhalation using a Borg scale ranging from 0 (no urge-to-cough) to 10 (most intense urge imaginable). The first concentration to elicit a perceptible level of urge-to-cough was denoted as the urge-to-cough threshold (C_u), and the first concentration to elicit two coughs was denoted as the cough threshold (C_2). Participants inhaled two concentrations above the C_2 threshold to assess tolerability prior to progressing to fMRI scanning. The same procedure of serial tidal breaths was undertaken with inhalations of doubling concentrations of ATP. However, in the event that two coughs were not elicited, participants inhaled the full range of concentrations to record associated levels of urge-to-cough and assess tolerability.

Four different concentrations of capsaicin and four different concentrations of ATP were then inhaled by participants during tidal breaths on two occasions for each concentration level in pseudorandom order, during which cough frequency and urge-to-cough ratings were recorded. The four concentrations of

capsaicin were the C2 dose (D2), one level below C2 (D1), one level above C2 (D3) and two concentration increments above C2 (D4). The second concentration in the incremental levels of ATP was a dose that had elicited an urge-to-cough rating that was the same as the participant's level of urge-to-cough reported in association with the C2 dose of capsaicin. This procedure was instituted to allow for comparisons between responses to the two substances that had equivalence along the stimulus-response relationship.

Further challenges with capsaicin and ATP were undertaken to estimate concentrations required for stimulation during fMRI data acquisition. Repeated inhalations of substances during scanning occurred in blocks of 24 seconds, during which the objective was to elicit an ongoing experience of an urge-to-cough and the absence of any coughing (Mazzone *et al.*, 2007a; Farrell *et al.*, 2012; Farrell *et al.*, 2014).

Participants were explicitly instructed to avoid coughing during 24-second inhalations of capsaicin and ATP in the psychophysical session. Increasing concentrations were used in successive trials to determine the maximum level that could be repeatedly inhaled without any instances of coughing. The concentration determined through this procedure was called the maximum suppressible dose (S_{\max}).

Stimulus Delivery and Behavioural Responses During Brain Imaging

Participants lay on the scanner bed with their heads stabilized with foam padding, and wearing earplugs for hearing protection. A mirror attached to the head coil provided line of sight to visual stimuli on a screen outside the scanner beyond participants' heads. Cotton wadding was used to prevent nasal breathing. A mask connected to three nebulisers was placed over participants' nose and mouth for delivery of capsaicin, ATP or saline. Functional brain imaging scans incorporated eight stimulus blocks, each of 24-seconds duration. Nebulised saline was inhaled during two stimulus blocks, and nebulised capsaicin and ATP solutions were inhaled three times each. The pseudorandom orders of stimuli differed between four fMRI scanning runs during a session but were replicated across participants. Participants received a "prepare" visual cue three seconds prior to the onset of each inhalation period. They were instructed to initiate inhalation when the prepare cue disappeared from the screen. Visual prompts for ratings of urge-to-cough appeared seven seconds after the conclusion of each stimulus block. Participants were instructed to use the fingers of both hands to indicate their ratings of urge-to-cough on a scale of zero to ten. There was a 37 second interval between the conclusion of one stimulus block and the onset of the subsequent block.

MRI Image Acquisition

Anatomical and functional brain images were acquired at Monash Biomedical Imaging, Clayton, Australia using a Siemens Skyra 3T scanner (Siemens Healthineers, Erlangen, Germany) and a 32-channel head coil. High-resolution T1-weighted images were acquired with 192 sagittal slices of 1 mm thickness and 1 x 1 mm² in-plane resolution in a matrix of 240 x 256, with an echo time (T_E) of 2.07 ms, a repetition time (T_R) of 1900 ms, an inversion time of 900 ms, and flip angle of 9°. Four fMRI acquisitions during each scanning session included two scans of the whole brain and two scans optimised for the brainstem. Whole brain echo planar images were acquired with 34 axial slices of 4.5 mm thickness, and in-plane resolution of 3.0 x 3.0 mm² in a matrix of 64 x 64. The 252 volumes in each of the two whole brain functional images had a T_R of 1950 ms, a T_E of 31 ms, and a flip angle of 90°. Brainstem echo planar images had 21 coronal oblique slices of 2.6 mm thickness aligned with the dorsal surface of the brainstem and a phase encoding direction of foot to head. The slices had 1.8 x 1.8 mm² in-plane resolution and a matrix of 106 x 106 that constituted a field of view (FOV) of sufficient size to incorporate a portion of the brain hemispheres rostral to the brainstem. Acquisition of 269 volumes per scan occurred with a T_R of 1930 ms, a T_E of 31 ms, and a flip angle of 90°. An additional image with the same slice orientation and similar acquisition parameters as brainstem functional images was obtained, but included 70 slices to achieve whole brain coverage for registration purposes ($T_R = 6370$ ms). Phase and magnitude images of the B_0 field were acquired for the generation of fieldmaps ($T_R=638$ ms, $T_{E1}=4.92$ ms $T_{E2}=7.38$ ms, 60 slices of 3 mm thickness, matrix 64x64, FOV=192 mm).

Data Processing and Statistical Analyses

Behaviour

Statistical analysis of behavioural measures was performed with SPSS 22.0. Values for C2, Cu and S_{max} were log transformed for the calculation of geometric means. Urge-to-cough ratings and cough frequencies recorded during the psychophysical session were tested for the effects of stimulus type (Capsaicin, ATP), concentration (four levels), and their interaction using repeated measures ANOVA and post hoc pairwise t-tests. Urge-to-cough ratings collected during scanning were tested for the effects of stimulus (Capsaicin, ATP), between-scan order (four scans), within-scan order (three stimulus blocks), and their interactions with repeated measures ANOVA. A mean urge-to-cough level during whole brain and brainstem scans for each participant was calculated for capsaicin and ATP stimulus blocks, and difference scores calculated between the two stimulus types. Coefficients of variation were calculated using the group means and standard deviations of the absolute numbers of the difference scores.

Pre-processing of Brain images

Analysis of functional brain images was performed with FSL (FMRIB's software library), including the FSL Expert Analysis Tool (FEAT, version 6.00). Whole brain functional images were realigned to the middle image of the time series using a six-parameter, rigid body method (MCFLIRT) (Jenkinson *et al.*, 2002), stripped of non-brain voxels with the brain extraction tool (BET) (Smith, 2002), spatially smoothed with a Gaussian kernel of 6.0 mm³ full width at half maximum, and high pass temporally filtered with a cut-off of 0.01 Hz. Registration of functional images to a common space was a two-stage process that involved alignment with participants' T1-weighted images using the Boundary-Based Registration (BBR) FSL tool (Greve & Fischl, 2009), and warping of the T1-weighted images to the Montreal Neurosciences Institute template brain (2.0mm³ isotropic voxels) (Fonov *et al.*, 2009), using FLIRT with 12 degrees of freedom (Jenkinson & Smith, 2001; Jenkinson *et al.*, 2002). The multiplication of the two registration matrices was used to transform outcomes of statistical analyses to a common space for the calculation of group effects.

Brainstem functional images were aligned with the middle image of the time series (MCFLIRT) (Jenkinson *et al.*, 2002), corrected for spatial distortion using fieldmaps and FMRIB's Utility for Geometrically Unwarping EPIs (FUGUE) (Jenkinson, 2003), spatially smoothed with a Gaussian kernel of 4.0 mm³ full width at half maximum, and high pass filtered with a cut-off of 0.01 Hz. Registration of images was a three-stage process. Firstly, the whole brain images acquired with similar slice orientation to the functional images were corrected for spatial distortion with FUGUE, stripped of non-brain voxels with BET, and used as the target image for alignments with functional images. Secondly, the stripped, FUGUE corrected whole brain images were registered to participants' T1-weighted images. Finally, T1-weighted images were warped to an MNI template brain with 1.0 mm³ isotropic voxels. The final step included a brainstem mask to weight registration of the brainstem region. Multiplication of the three matrices was used to transform statistical parametric maps from native to standard space for analysis of group effects.

Analysis of BOLD Signal Changes in the Hemispheres of the Brain

General linear modelling of individual time series BOLD data from the whole brain images was carried out with local autocorrelation correction (Woolrich *et al.*, 2001). Experimental events were represented with regressors that were convolved with a gamma hemodynamic response function. These events included the timing of inhaled stimuli (capsaicin, ATP, saline), as well as visual cues and rating tasks. Temporal

derivatives of experimental events were also included as regressors in the models of BOLD signal changes.

The six motion parameters (three translations, three rotations) were included as confound variables.

Additional confound variables were included that have been shown to reduce the influence of respiratory-related noise to the calculation of effects associated with experimental events (Birn *et al.*, 2008; Birn *et al.*, 2009). This strategy is indicated when events of interest are likely to correlate with respiratory function, as was the case for this study. The additional confounds included signals extracted from the BOLD time series in regions including the white matter, ventricles, and a noisy voxel with high levels of variance. The standard deviations of the time series were calculated, and the resulting images were thresholded to identify the noisiest voxel. This voxel was typically between the hemispheres in a region likely to incorporate the sagittal sinus in the whole brain images (Farrell *et al.*, 2012). An additional confound variable was included that represented global signal changes in non-activated voxels. A preliminary group analysis was undertaken to identify voxels with responses to any one of the three airway stimuli, and these voxels were excluded from a mask that was used to calculate the modified global signal variance across the time series. This approach is used to further characterise changes in BOLD signal due to respiratory-related noise (Mazzone *et al.*, 2011; Farrell *et al.*, 2012), and was first advocated as a strategy to model global effects while excluding the contribution of activation to this variance (Andersson, 1997).

Contrasts of parameter estimates (COPE) for effects associated with the inhaled stimuli were performed to show voxels with signal changes during capsaicin and ATP inhalations that were increased compared to saline inhalations (Capsaicin > Saline, ATP > Saline). Additional contrasts tested for differences between the two tussive stimuli (Capsaicin > ATP, ATP > Capsaicin). Statistical parametric maps representing COPEs were transformed to standard space for higher level analyses. The second level involved the calculation of average effects within each participant's data, modelled as fixed effects. Outcomes of the second level analyses were inputs into group analyses that modelled between-participant variance as mixed effects. Additional regressors were included in one whole brain group analysis to test for associations between behavioural outcomes and regional activation levels. This analysis involved difference scores between urge-to-cough ratings for ATP and capsaicin as predictors of variance in COPE levels for the contrast of Capsaicin > ATP). Group effects were thresholded to include voxels with values of $z > 3.1$ and forming contiguous clusters with a probability threshold $p < 0.05$, corrected for multiple comparisons based on Gaussian random field theory (Worsley *et al.*, 1992).

Region of interest (ROI) analyses were performed to characterise outcomes of the whole brain group analyses. Masks were created of voxels in activated clusters that were in uniform neuroanatomical structures according to the Harvard-Oxford structural atlas (Desikan *et al.*, 2006). These masks were defined for the outcomes of Capsaicin > ATP, and those regions of this contrast that showed an association with urge-to-cough difference scores. The masks were used with Featquery to calculate percentage signal changes of ROI for primary effects (Capsaicin > Saline, ATP > Saline). Estimates of percentage signal change were averaged across the two scan outcomes for each individual participant, and subsequently used to show effects of stimulus type (paired t-tests), and associations between differences in stimulus-related activation and urge-to-cough difference scores (Pearson correlations).

Analysis of BOLD Signal Changes in the Brainstem

General linear modelling of BOLD signal changes in brainstem images followed similar processes to the analysis of the data from the hemispheres of the brain. Regressors representing the events in the experimental model were convolved with a gamma hemodynamic response function. The range of confounds used in the modelling of brainstem BOLD signal changes was the same as the hemispheres, but the location of the noisiest voxel differed for the two regions. Unlike the noisiest voxels in the hemispheres, which were usually in the sagittal sinus, voxels with high levels of noise in brainstem images frequently appeared in regions likely to be in the carotid circulation (Bautista *et al.*, 2019a). Contrasts of parameter estimates for Capsaicin > Saline and ATP > Saline were transformed to standard space for averaging across runs within participants (fixed effects), the results of which were inputs into a mixed effects analysis to identify group results. The brainstem statistical parametric maps for Capsaicin > Saline and ATP > Saline were thresholded with the less stringent voxel inclusion of $z > 2.3$, and a cluster corrected threshold of $p < 0.05_{\text{corrected}}$. This approach was used in recognition of the lower levels of signal to noise ratios in the functional brainstem images that reflects the need for smaller voxels (less signal) to localise activation in relatively small structures (medullary nuclei) in a region of the brain that is likely to show movements related to physiological parameters (increased noise). The group results of the Capsaicin > Saline and ATP > Saline contrasts were used to illustrate the neuroanatomical locations of activated regions, and to inform a region of interest analysis that tested for the independent and interacting effects of stimulus type (Capsaicin, ATP), region (NTS, Pa5) and side (Left, Right).

Tests of brainstem activations were based on a region of interest approach with the respective responses of the NTS and Pa5 the focus of this assessment. The rationale for this approach was based on strong priors

for the critical role of these nuclei in the initial processing of inputs from the airways (Driessen *et al.*, 2015; McGovern *et al.*, 2015a; McGovern *et al.*, 2015b; Driessen *et al.*, 2018; Bautista *et al.*, 2019b; Driessen *et al.*, 2020). The tussive stimuli used in the experiment were expected to produce differential responses in the NTS and Pa5 based on the assumption of homology between humans and the rat and guinea pig. Homology would be demonstrated if responses to capsaicin were observed at both nuclei (NTS and Pa5) and ATP responses were seen in the NTS alone. In order to test this assumption an analysis of variance (ANOVA) in BOLD signal changes from regions of interest was planned. The interaction term of an ANOVA incorporating region (NTS, Pa5) and stimulus (Capsaicin, ATP) factors is an estimate of the effect with greatest relevance for the hypothesised differential responses of the nuclei to the tussive stimuli, which would not be feasible with standard voxel-wise analyses that preclude tests of inter-regional effects. The target regions were chosen as the likely sites of the NTS, and the Pa5. Localisations were based on neuroanatomy, activation outcomes of the study reported here, and past experience with functional brainstem imaging of responses to inhalation of tussive stimulation. Neuroanatomy was informed by reference to a brainstem atlas (Paxinos *et al.*, 2012). The atlas incorporated slices that were axial in orientation and configured according to the distance from the obex at 1.0 mm intervals. Atlas slices were perpendicular to the long axis of the brainstem, and consequently were not parallel to the line between the anterior commissure and posterior commissure, which is the case for the standard template brain used for image registration. The estimates of the corresponding levels between the atlas and standard brain were made according to proximity of the obex, with adjustments based on the relative distances between the obex and the caudal margin of the aqueduct (the standard brainstem is longer than the atlas brainstem, see (Bautista *et al.*, 2019a)). The estimated locations of the two nuclei as indicated by the atlas were inspected visually after rendering the outcomes of the contrasts of Capsaicin > Saline and ATP > Saline to identify the most proximate peaks of activation. Two masks were drawn to include four contiguous voxels (4.0 mm³) with the highest statistic values for Capsaicin > Saline in the dorsolateral locations of the left and right Pa5 as indicated by the atlas. The locations of these masks in the axial slices were at z=-58 in the MNI brainstem, near the obex in the standard space. The NTS spans a substantial extent of the medulla in the rostrocaudal direction. Our previous study of BOLD signal changes in the brainstem associated with capsaicin inhalation showed a symmetrical dorsal activation extending either side of the midline in an axial slice of z=-54, a location likely to incorporate the NTS. Two masks, each of the four highest Capsaicin > Saline statistic values in the z=-55 slice, were made either side of the midline to represent the left and right NTS. The four masks (left and right Pa5, left and right NTS) were used with Featquery to estimate the percentage BOLD signal changes for the Capsaicin > Saline and ATP > Saline contrasts for each scanning run of brainstem images from all participants. These values were dependent variables in a repeated measures ANOVA to test the effects of nuclei (Pa5, NTS), stimulus type (Capsaicin,

ATP), side (Left, Right) and their interactions. Post hoc paired t-tests were planned to characterise any significant effects resulting from the ANOVA.

Author Manuscript

Results

Behavioural Responses to Inhalation of Capsaicin and ATP

The logarithms of levels of the Cu, C2 and S_{\max} thresholds for both capsaicin and ATP for each participant are displayed in figure 1A. The geometric mean levels of the capsaicin thresholds for Cu were -0.89 ± 0.41 , for C2 were -0.04 ± 0.43 , and for S_{\max} were -0.60 ± 0.58 . The geometric mean Cu and S_{\max} thresholds for ATP were 0.76 ± 0.58 and 1.76 ± 0.50 respectively. C2 thresholds for ATP were not determined for fifteen participants who did not cough to any of the challenge concentrations. The geometric mean of the C2 thresholds for the five participants who coughed to ATP was 1.64 ± 0.58 . Tests for sex-related differences were not significant for any of the threshold levels (p values ranged from $p=0.71$ to $p=0.46$). Urge-to-cough ratings associated with S_{\max} inhalations did not show significant differences between capsaicin and ATP ($t(19)=1.5$, $p=0.2$, Capsaicin 3.2 ± 1.5 , ATP 3.6 ± 1.7), and were notable for high levels of variability between the two tussive stimuli within participants (coefficient of variation = 79%).

Concentration (four levels) was a significant factor in variance of urge-to-cough ratings for responses to the challenges with the two substances ($F(3,57)=77.5$, $p<0.001$) (Figure 1B). Stimulus (Capsaicin, ATP) was not a significant factor ($F(1,19)=0.7$, $p=0.4$), nor was there an interaction with concentration for urge-to-cough ratings ($F(3,57)=0.003$, $p=1$) during the psychophysical session. Both concentration ($F(3,57)=39.2$, $p<0.0001$) and stimulus ($F(1,19)=17.0$, $p<0.001$) were significant factors for cough frequency in response to the tussive challenges (Figure 1C). Coughing was more frequent for capsaicin challenges compared to ATP challenges (Capsaicin 0.74 ± 0.56 , ATP 0.17 ± 0.31). The two factors interacted ($F(3,57)=9.7$, $P<0.001$), with higher concentrations showing the most pronounced differences between the two stimulus types.

Tachyphylaxis, which can be a feature of repeated inhalation of capsaicin (Mazzone *et al.*, 2007b), was not observed for either stimulus type during the collection of brain images. There was an absence of significant changes in urge-to-cough ratings during the whole brain imaging associated with the order of the two functional scans ($F(1,19)=3.8$, $p=0.07$), the order of stimulus block within scans ($F(2,38)=1.9$, $p=0.2$), and the stimulus type (ATP versus Capsaicin, $F(1,19)=0.03$, $p=0.9$), nor were there any significant interactions between the factors. The same factors also showed an absence of significant effects for the urge-to-cough ratings during the brainstem imaging (scan order $F(1,19)=0.5$, $p=0.5$, stimulus block order $F(2,38)=0.5$, $p=0.6$, stimulus type $F(1,19)=0.1$, $p=0.8$), nor were there any significant interactions between the factors. The respective levels of urge-to-cough reported in response to capsaicin and ATP challenges during scanning were widely variable among the participants (Figure 1D). While the average urge-to-cough

ratings approximated for the two stimuli during scanning (whole brain, Capsaicin 4.0 ± 1.9 , ATP 3.9 ± 1.7 , brainstem, Capsaicin 3.7 ± 2.1 , ATP 3.9 ± 1.9), the mean of the absolute numbers of differences between the stimuli were 1.8 ± 1.0 during whole brain imaging and 1.9 ± 1.5 during brainstem imaging, which constitute coefficients of variation of 55% and 75% respectively.

Regional Brain Responses to Capsaicin and ATP Inhalation

BOLD Signal Changes Associated with Tussive Stimuli in Brainstem Regions

The locations of activations for Capsaicin>Saline and ATP>Saline are shown in figures 2 and 3. Capsaicin>Saline activation was distributed throughout the dorsal extent of the caudal medulla encompassing the ROI likely to include the Pa5 and NTS. The cluster of ATP>Saline activation in the caudal medulla was not as extensive as Capsaicin>Saline, and was generally confined to the dorsomedial location that included the NTS ROI. A lateral, asymmetrical extension of the ATP>Saline cluster was seen on the right side of medulla, but this region was mesial and ventral relative to the ROI used to extract signals from the Pa5. Stimulus type was not a significant factor in the variance of BOLD signal intensity changes in response to tussive challenges greater than saline inhalations from ROI in the medulla (Capsaicin versus ATP, $F(1,19)=4.0$, $p=0.06$). There was also an absence of significant differences for the contrasts of dorsolateral versus dorsomedial regions ($F(1,19)=2.2$, $p=0.2$), and left versus right sides ($F(1,19)=0.01$, $p=0.8$). However, there was a significant interaction between stimulus type and regional location ($F(1,19)=13.0$, $p<0.002$) (Figure 2). Post hoc paired t-tests showed significant stimulus type-related differences for the dorsolateral regions on the left (%BOLD signal change - Capsaicin 0.34 ± 0.3 , ATP 0.04 ± 0.6 , $t(19)=2.8$, $p<0.02$) and on the right (%BOLD signal change - Capsaicin 0.36 ± 0.5 , ATP 0.08 ± 0.5 , $t(19)=3.3$, $p<0.004$). Similar contrasts for the dorsomedial regions were not significant for the left (%BOLD signal change - Capsaicin 0.3 ± 0.4 , ATP 0.3 ± 0.5 , $t(19)=0.2$, $p=0.9$) and right sides (%BOLD signal change - Capsaicin 0.3 ± 0.4 , ATP 0.3 ± 0.5 , $t(19)=0.5$, $p=0.6$). There were no further significant interactions between the factors.

Regions above the caudal medulla in the brainstem showing activation for the contrasts of Capsaicin > Saline and ATP > Saline were co-localised. Figure 3 is a logical map that shows extensive overlaps of the activation for the two stimulus types in the dorsal rostral medulla, dorsal pons, and rostral midbrain.

Capsaicin and ATP-Related Activations in Hemispheres of the Brain

Responses for Capsaicin>Saline and ATP>Saline were widely distributed throughout similar regions of the hemispheres of the brain (see Figure 4). These regions included the superior frontal gyrus, supplementary motor area, premotor cortices, dorsolateral prefrontal cortex, mid-cingulate cortex, posterior parietal cortex, primary somatosensory and motor cortices including Rolandic regions, insula, thalamus, caudate, putamen and cerebellum ($p_{\text{corrected}} < 0.05$) (see Table 1 for details).

Associations of Urge-to-Cough with Differences between Capsaicin and ATP Activations

Notable levels of within subject variance were observed for ratings of urge-to-cough for the respective stimulus types during scanning (see earlier section *Behavioural Responses to Inhalation of Capsaicin and ATP* and figure 1D). A difference score of urge-to-cough ratings between Capsaicin and ATP scanning periods was calculated for each participant and used as a regressor to test for associations with the complementary imaging contrast of Capsaicin>ATP. The outcome of this correlation analysis was masked to only include those voxels that showed activation for the conjunction of the contrasts of Capsaicin>Saline and ATP>Saline. Regions showing activation levels for the Capsaicin>ATP contrast that were correlated with variance among participants in stimulus-related urge-to-cough differences included superior frontal gyrus, supplementary motor region, mid cingulate cortex, premotor cortices, middle frontal gyrus, pre/post central gyrus and operculum, insula, thalamus and cerebellum ($p_{\text{corrected}} < 0.05$) (see Figure 5 and Table 2).

Differences Between Capsaicin and ATP Activations

Contrasts of activations between the two tussive stimuli were undertaken in both directions and included differences in urge-to-cough ratings as covariates. Differences for the contrast of Capsaicin>ATP were observed in brain regions including premotor cortex, supplementary motor area, central operculum, anterior insula, inferior frontal gyrus and cerebellum ($p_{\text{corrected}} < 0.05$) (Figure 6 and Table 3). Examination of BOLD signal changes from the regions showing differences for Capsaicin>ATP indicated positive mean changes of all regions for both stimuli that were significantly increased during capsaicin inhalation compared to ATP inhalation (Figure 6). The contrast of ATP>Capsaicin did not show any significant regions of activation.

Discussion

In the present study we utilized inhaled stimuli shown, using electrophysiological studies in animals, to have differential efficacy for activating jugular and nodose vagal afferents (Kwong *et al.*, 2008; Mazzone & Udem, 2016; Kollarik *et al.*, 2019), with the aim of further defining the bulbar and higher brain processing pathways for different respiratory sensory inputs in healthy adults. Inhalation of ATP selectively activated a dorsomedial medullary region that included the NTS, whereas inhalation of capsaicin was associated with activation in both dorsomedial and dorsolateral medullary regions encompassing to the NTS and Pa5. Levels of regional BOLD signal responses were also increased for capsaicin compared to ATP in the hemispheres of brain, principally in regions ascribed with motor control functions. These observed regional brain responses may be related to behavioural differences between the respective tussive stimuli in cough frequency.

Evidence for multiple neural circuits processing respiratory sensations

Two embryologically distinct populations of vagal afferent neurons innervate the airways and lungs (Mazzone & Udem, 2016), suggestive of underappreciated complexity in the neural processes governing respiratory sensations. In laboratory animals, both the jugular and nodose vagal ganglia contribute chemically-sensitive nociceptor innervation to the respiratory tree, although important differences exist in the physiology and anatomy of these two ganglia populations. Notably, in mice and guinea pigs, both jugular and nodose nociceptors are robustly activated by capsaicin and other activators of TRPV1, whereas only neurons from the placode-derived nodose ganglia express functional heteromeric P2X2/3 purinergic receptors needed for ATP responsivity (Kwong *et al.*, 2008; Mazzone & Udem, 2016). Furthermore, we have previously shown in rats and guinea pigs that jugular and nodose vagal afferents terminate centrally in non-overlapping medullary regions of the Pa5 and the NTS, respectively (Driessen *et al.*, 2015; McGovern *et al.*, 2015a; McGovern *et al.*, 2015b; Driessen *et al.*, 2018). Given these observations, we reasoned that if the same neurophysiological and neuroanatomical organization is true for human vagal afferents, then differential patterns of activation in the human brainstem should be observed following inhaled challenges with capsaicin compared to ATP. More specifically, neural responses evoked by the nodose-selective stimulus ATP should be spatially restricted within a more distributed pattern of activity evoked by capsaicin, because the latter would include regional neural processes activated by both nodose and jugular afferent inputs.

Our brainstem imaging data are entirely consistent with the pattern of activation predicted during capsaicin and ATP challenges. Thus, capsaicin evoked significant increases in BOLD signal in the dorsal half of the caudal medulla, near the level of the Obex, that extended bilaterally from the midline to the lateral borders of the medulla. At this rostrocaudal level, the regions of activation incorporate the medially-located NTS, well known to receive nodose afferent inputs, and the laterally-located trigeminal (including Pa5) areas receiving inputs from jugular vagal afferents (Driessen *et al.*, 2015; McGovern *et al.*, 2015b; Driessen *et al.*, 2018), both of which respond to capsaicin inhalation in humans (Bautista *et al.*, 2019a). By contrast, at the same rostrocaudal medullary levels the bulbar activations induced by the putatively nodose-selective stimulus ATP were restricted to medially-located regions of the medulla, consistent with sensory integration confined to the NTS. To our knowledge, this is the first neurophysiological data in humans to support the existence of anatomically distinct parallel vagal afferent pathways involved in the processing of any visceral sensation.

The presence of two medullary processing nuclei for incoming respiratory sensory inputs suggests that nodose and jugular vagal neurons might regulate distinct ascending central sensory circuits. Using conditional transynaptic viral tracing, we previously provided evidence in rodents that the higher order subcortical processing regions in receipt of nodose and jugular inputs do in fact differ. Nodose airway afferent pathways integrate extensively into central limbic and autonomic circuits while jugular airway afferent pathways resemble those involved in somatosensation (McGovern *et al.*, 2015b). In the present study we confirmed again the functional organization of the distributed higher brain network activated by capsaicin inhalation in humans, in which regional BOLD signal responses are consistently observed in localised areas of the insula, somatosensory, cingulate, prefrontal and parietal cortices. Furthermore, we showed that ATP inhalation evoked activations that were localized entirely within this broader airway nociceptor-activated network. Predictably, there were no regional responses unique to ATP, indicative of the nodose afferent processing neural network residing within the general nociceptor network activated by capsaicin. Conversely, regional response unique to capsaicin were identified, which may provide insight into some unique aspects of jugular afferent processing in the brain.

Distinct contributions of jugular and nodose vagal afferents to cough sensory processing

The relative contribution of nodose and jugular airway afferent pathways in the genesis of cough and the urge-to-cough is not known. In experimental studies, stimuli (such as capsaicin) that activate both jugular and nodose vagal chemically-sensitive afferents evoke cough and perceptions of airway irritation in

conscious animals and humans, whereas stimuli selective for nodose neurons (such as serotonin, adenosine and ATP) produce appreciably less coughing. Indeed, in guinea pigs, nodose-selective stimuli have been shown to inhibit cough evoked by other tussive stimuli (Chou *et al.*, 2018). Consistent with these observations, we saw significantly less coughing in our healthy human participants in response to ATP challenges, when compared to that evoked by capsaicin. Nevertheless, ATP did evoke perceivable and unpleasant sensations consistent with airway afferent activation. These sensations were described and rated as an 'urge-to-cough' and were evoked at subjectively comparable magnitudes to those induced by capsaicin. This may argue that even though nodose-selective stimuli are poor tussigens, nodose afferents still provide input to central neural circuits involved in respiratory sensory discrimination and affect encoding. Important to this concept, however, is whether the nature of the perceived sensory experience is comparable between nodose and jugular afferent stimuli. Our studies were not designed to assess this, although anecdotally our participants reported capsaicin-evoked sensations confined to laryngeal regions compared to ATP-evoked sensations that were more diffusely distributed in the chest. In guinea pigs, jugular and nodose nociceptors predominate in the extrapulmonary and intrapulmonary airways, respectively (McGovern *et al.*, 2015a), and ATP may activate non-nociceptor nodose afferent populations as well (Mazzone & Udem, 2016). This anatomical and functional heterogeneity could give rise to different sensory experiences, depending on the afferent population(s) activated. Perhaps consistent with this, in humans we have shown that discriminative processing of bronchopulmonary sensory inputs involves multiple cortical networks, in which activations in the insula cortex are aligned with encoding the magnitude of the airway stimulus, whereas those in the primary somatosensory cortex correlate closely with perceptual ratings of the urge-to-cough (Farrell *et al.*, 2012). Unfortunately, the lack of any jugular-selective airway nociceptive stimuli limits our current capacity to investigate this more rigorously.

Limitations of the study

The fMRI protocol involved inhaling capsaicin or ATP for 24s, necessary for optimal BOLD signal activation using our established block stimulus design (Mazzone *et al.*, 2007a; Farrell *et al.*, 2012; Bautista *et al.*, 2019a), while the ratings of urge-to-cough provided by the participants were collected at the end of each challenge, as commonly performed to provide insight into the level of airway irritation evoked by each stimulus block. This was necessary to minimise confounding motor and cognitive tasks during challenge blocks, which would present additional sources of BOLD signal variances that would compromise our ability to discern responses relating to the stimulus alone. Consequently, this limitation in design means that only the average urge-to-cough evoked by capsaicin and ATP was collected for each stimulus block, and we cannot rule out the possibility that differences in breath by breath kinetics of the sensations evoked by the

different stimuli during each 24 second block exists, perhaps reflective of differences in stimulus tachyphylaxis, disproportionate primary afferent encoding of the stimuli or more complex differences in higher order sensory processing. Participant verbal reports are not consistent with substantive differences in sensory kinetics, and fMRI is unlikely to have temporal resolution to be impacted by subtle kinetic differences, but nevertheless this should be acknowledged as a contributing factor to the differences noted between capsaicin and ATP in brainstem and brain BOLD signal responses. Additionally, it is conceivable that capsaicin and ATP could functionally interact when inhaled repeatedly, and this could also confound fMRI data. Importantly, no significant interactions between stimulus order and urge-to-cough were noted, again providing support that substantive effects of this kind are unlikely. Furthermore, previous studies in guinea pigs and humans have shown that ATP does not alter capsaicin cough responsiveness (Kamei *et al.*, 2005; Basoglu *et al.*, 2017).

Comparison of brainstem activation patterns suggests more widespread BOLD signal changes evoked by capsaicin compared to ATP, most notable in more caudal medullary slices (e.g., $z=-58$). As such, capsaicin evoked BOLD signal changes not only encompass the predicted nTS and Pa5 regions of the medulla but extend to include neighbouring regions of the reticular brainstem, and spinal trigeminal nucleus. The reason for this more expansive activation pattern is not entirely clear. It is possible that stimulus concentrations of capsaicin and ATP are not functionally equivalent. Thus, although we chose capsaicin and ATP concentrations that effectively produced equivalent levels of urge-to-cough, overall sensory nerve activity may not be identical and capsaicin-sensitive afferent pathways in general may be more active than ATP-sensitive pathways. However, if true, this would provide additional evidence of two parallel urge-to-cough sensory systems with distinct central wiring. Alternatively, inhaled capsaicin may activate broader subsets of medullary projecting afferents compared to ATP, potentially including afferents of both vagal and non-vagal origin. Indeed, oropharyngeal afferents of the trigeminal system may be activated by substances when inhaled via the mouth and to this end we have previously reported oropharyngeal sensory experiences in our participants when challenged with inhaled (mouth breathing) capsaicin (Mazzone *et al.*, 2007a). However, when experienced, such sensations are persistent, reported by participants as an ongoing low-level sense of burning in the mouth that does not abate for the duration of the experiment. This is starkly different to the transient 'on-off' sense of urge-to-cough that we use to model the BOLD signal activity associated with laryngeal and airway irritation. As such, any BOLD signal changes resulting from persistent activations arising from the oropharynx are already excluded from the BOLD signals reported in the present study. It is also conceivable that nodose and jugular vagal afferents have differences in either their density and extent of central projections and/ or the extent of connectivity

with other bulbar networks, which could contribute to the differences seen between capsaicin and ATP evoked BOLD signal changes in the caudal medulla. Neuroanatomical tracing studies in laboratory animals lends some support this assertion (McGovern et al., 20015a,b). However, the temporal resolution of our fMRI protocol does not allow for first-order and higher-order network activity to be untangled and as such this remains speculative. It is also intriguing that in the rostral medulla and pons, the apparent differences between capsaicin and ATP evoked activity are less notable, suggesting similar regional network activity in more rostral brainstem sites.

Conclusions and clinical implications

The present data provide support for the existence of multiple, parallel vagal afferent pathways subserving respiratory sensory processing. In the clinical setting, chronic cough contributes significantly to patient morbidity in over 100 clinical conditions and patients report that changes in ambient temperature, laughing, talking on the phone for more than a few minutes, aerosol sprays, or smoky atmospheres trigger their coughing (Mazzone *et al.*, 2018). This argues strongly for a state of sensory hypersensitivity as a common pathophysiological characteristic. However, it remains unclear as to the relative contribution of jugular and nodose vagal afferent pathways in the development of cough hypersensitivity. Intriguingly, recent clinical trials with an ATP blocking P2X3 antagonist show promise for reducing cough (Abdulqawi *et al.*, 2015), which may point to a prominent role for nodose afferents and central processing via bulbar circuits involving the NTS. However, P2X3-dependent responses might become upregulated in jugular afferents. Thus, it will be important to understand how central neural responses induced by inhaled ATP challenge change in patients with chronic cough, as this may provide important insight into the neural processes that govern the development of cough sensitization.

References

- Abdulqawi R, Dockry R, Holt K, Layton G, McCarthy BG, Ford AP & Smith JA. (2015). P2X3 receptor antagonist (AF-219) in refractory chronic cough: a randomised, double-blind, placebo-controlled phase 2 study. *Lancet (London, England)* **385**, 1198-1205.
- Andersson JL. (1997). How to estimate global activity independent of changes in local activity. *NeuroImage* **6**, 237-244.
- Ando A, Farrell MJ & Mazzone SB. (2014). Cough-related neural processing in the brain: a roadmap for cough dysfunction? *Neuroscience and biobehavioral reviews* **47**, 457-468.
- Baker C. (2005). Vertebrate cranial placodes I. Embryonic induction. In *Advances in Vagal Afferent Neurobiology*, ed. Udem BJ aWD. CRC Taylor and Francis, Boca Raton FL.
- Basoglu OK, Pelleg A, Kharitonov SA & Barnes PJ. (2017). Contrasting effects of ATP and adenosine on capsaicin challenge in asthmatic patients. *Pulmonary pharmacology & therapeutics* **45**, 13-18.
- Bautista TG, Leech J, Mazzone S & Farrell MJ. (2019a). Regional brainstem activations during capsaicin inhalation using functional magnetic resonance imaging in humans. *Journal of neurophysiology* **121**(4):1171-1182.
- Bautista TG, Leech J, Mazzone SB & Farrell MJ. (2019b). Regional brain stem activations during capsaicin inhalation using functional magnetic resonance imaging in humans. *Journal of Neurophysiology* **121**, 1171-1182.
- Birn RM, Murphy K, Handwerker DA & Bandettini PA. (2009). fMRI in the presence of task-correlated breathing variations. *NeuroImage* **47**, 1092-1104.
- Birn RM, Smith MA, Jones TB & Bandettini PA. (2008). The respiration response function: the temporal dynamics of fMRI signal fluctuations related to changes in respiration. *NeuroImage* **40**, 644-654.

- Chou YL, Mori N & Canning BJ. (2018). Opposing effects of bronchopulmonary C-fiber subtypes on cough in guinea pigs. *American journal of physiology Regulatory, integrative and comparative physiology* **314**, R489-r498.
- D'Autreaux F, Coppola E, Hirsch MR, Birchmeier C & Brunet JF. (2011). Homeoprotein Phox2b commands a somatic-to-visceral switch in cranial sensory pathways. *Proceedings of the National Academy of Sciences of the United States of America* **108**, 20018-20023.
- Davenport PW. (2009). Clinical cough I: the urge-to-cough: a respiratory sensation. *Handbook of experimental pharmacology*, 263-276.
- Desikan RS, Segonne F, Fischl B, Quinn BT, Dickerson BC, Blacker D, Buckner RL, Dale AM, Maguire RP, Hyman BT, Albert MS & Killiany RJ. (2006). An automated labeling system for subdividing the human cerebral cortex on MRI scans into gyral based regions of interest. *NeuroImage* **31**, 968-980.
- Driessen AK, Farrell MJ, Dutschmann M, Stanic D, McGovern AE & Mazzone SB. (2018). Reflex regulation of breathing by the paratrigeminal nucleus via multiple bulbar circuits. *Brain structure & function* **223**, 4005-4022.
- Driessen AK, Farrell MJ, Mazzone SB & McGovern AE. (2015). The Role of the Paratrigeminal Nucleus in Vagal Afferent Evoked Respiratory Reflexes: A Neuroanatomical and Functional Study in Guinea Pigs. *Frontiers in physiology* **6**, 378.
- Driessen AK, Farrell MJ, Mazzone SB & McGovern AE. (2016). Multiple neural circuits mediating airway sensations: Recent advances in the neurobiology of the urge-to-cough. *Respiratory physiology & neurobiology* **226**, 115-120.
- Driessen AK, McGovern AE, Behrens R, Moe AAK, Farrell MJ & Mazzone SB. (2020). A role for neurokinin 1 receptor expressing neurons in the paratrigeminal nucleus in bradykinin-evoked cough in guinea-pigs. *J Physiol*.

- Farrell MJ, Cole LJ, Chiapoco D, Egan GF & Mazzone SB. (2012). Neural correlates coding stimulus level and perception of capsaicin-evoked urge-to-cough in humans. *NeuroImage* **61**, 1324-1335.
- Farrell MJ, Koch S, Ando A, Cole LJ, Egan GF & Mazzone SB. (2014). Functionally connected brain regions in the network activated during capsaicin-inhalation. *Human Brain Mapping* **35**, 5341-5355.
- Fonov VS, Evans AC, McKinstry RC, Almlri CR & Collins DL. (2009). Unbiased nonlinear average age-appropriate brain templates from birth to adulthood. *NeuroImage* **47**, S39-S41.
- Fowles HE, Rowland T, Wright C & Morice A. (2017). Tussive challenge with ATP and AMP: does it reveal cough hypersensitivity? *The European respiratory journal* **49**.
- Greve DN & Fischl B. (2009). Accurate and robust brain image alignment using boundary-based registration. *NeuroImage* **48**, 63-72.
- Hilton E, Marsden P, Thurston A, Kennedy S, Decalmer S & Smith JA. (2015). Clinical features of the urge-to-cough in patients with chronic cough. *Respiratory medicine* **109**, 701-707.
- Jenkinson M. (2003). Fast, automated, N-dimensional phase-unwrapping algorithm. *Magnetic resonance in medicine* **49**, 193-197.
- Jenkinson M, Bannister P, Brady M & Smith S. (2002). Improved optimization for the robust and accurate linear registration and motion correction of brain images. *NeuroImage* **17**, 825-841.
- Jenkinson M & Smith S. (2001). A global optimisation method for robust affine registration of brain images. *Medical image analysis* **5**, 143-156.
- Kamei J, Takahashi Y, Yoshikawa Y & Saitoh A. (2005). Involvement of P2X receptor subtypes in ATP-induced enhancement of the cough reflex sensitivity. *European journal of pharmacology* **528**, 158-161.

- Kollarik M, Ru F & Udem BJ. (2019). Phenotypic distinctions between the nodose and jugular TRPV1-positive vagal sensory neurons in the cynomolgus monkey. *Neuroreport* **30**, 533-537.
- Kwong K, Kollarik M, Nassenstein C, Ru F & Udem BJ. (2008). P2X2 receptors differentiate placodal vs. neural crest C-fiber phenotypes innervating guinea pig lungs and esophagus. *American journal of physiology Lung cellular and molecular physiology* **295**, L858-865.
- Mazzone SB, Chung KF & McGarvey L. (2018). The heterogeneity of chronic cough: a case for endotypes of cough hypersensitivity. *The Lancet Respiratory medicine* **6**, 636-646.
- Mazzone SB, Cole LJ, Ando A, Egan GF & Farrell MJ. (2011). Investigation of the neural control of cough and cough suppression in humans using functional brain imaging. *The Journal of neuroscience : the official journal of the Society for Neuroscience* **31**, 2948-2958.
- Mazzone SB, McLennan L, McGovern AE, Egan GF & Farrell MJ. (2007a). Representation of capsaicin-evoked urge-to-cough in the human brain using functional magnetic resonance imaging. *American journal of respiratory and critical care medicine* **176**, 327-332.
- Mazzone SB, McLennan L, McGovern AE, Egan GF & Farrell MJ. (2007b). Representation of Capsaicin-evoked Urge-to-Cough in the Human Brain Using Functional Magnetic Resonance Imaging. *American Journal of Respiratory and Critical Care Medicine* **176**, 327-332.
- Mazzone SB & Udem BJ. (2016). Vagal Afferent Innervation of the Airways in Health and Disease. *Physiological reviews* **96**, 975-1024.
- McGovern AE, Davis-Poynter N, Yang SK, Simmons DG, Farrell MJ & Mazzone SB. (2015a). Evidence for multiple sensory circuits in the brain arising from the respiratory system: an anterograde viral tract tracing study in rodents. *Brain structure & function* **220**, 3683-3699.
- McGovern AE, Driessen AK, Simmons DG, Powell J, Davis-Poynter N, Farrell MJ & Mazzone SB. (2015b). Distinct brainstem and forebrain circuits receiving tracheal sensory neuron inputs revealed using a novel conditional anterograde transsynaptic viral tracing

system. *The Journal of neuroscience : the official journal of the Society for Neuroscience* **35**, 7041-7055.

Morice AH, Kitt MM, Ford AP, Tershakovec AM, Wu WC, Brindle K, Thompson R, Thackray-Nocera S & Wright C. (2019). The Effect of Gefapixant, a P2X3 antagonist, on Cough Reflex Sensitivity: A randomised placebo-controlled study. *The European respiratory journal*.

Nassenstein C, Taylor-Clark TE, Myers AC, Ru F, Nandigama R, Bettner W & Udem BJ. (2010). Phenotypic distinctions between neural crest and placodal derived vagal C-fibres in mouse lungs. *The Journal of physiology* **588**, 4769-4783.

Paxinos G, Huang XF, Sengul G & Watson C. (2012). Organisation of brainstem nuclei. In *The Human Nervous System*, ed. J. Mai GP, pp. 260-327. Academic, San Diego, CA.

Smith SM. (2002). Fast robust automated brain extraction. *Hum Brain Mapp* **17**, 143-155.

Woolrich MW, Ripley BD, Brady M & Smith SM. (2001). Temporal autocorrelation in univariate linear modeling of FMRI data. *NeuroImage* **14**, 1370-1386.

Worsley KJ, Evans AC, Marrett S & Neelin P. (1992). A three-dimensional statistical analysis for CBF activation studies in human brain. *Journal of cerebral blood flow and metabolism : official journal of the International Society of Cerebral Blood Flow and Metabolism* **12**, 900-918.

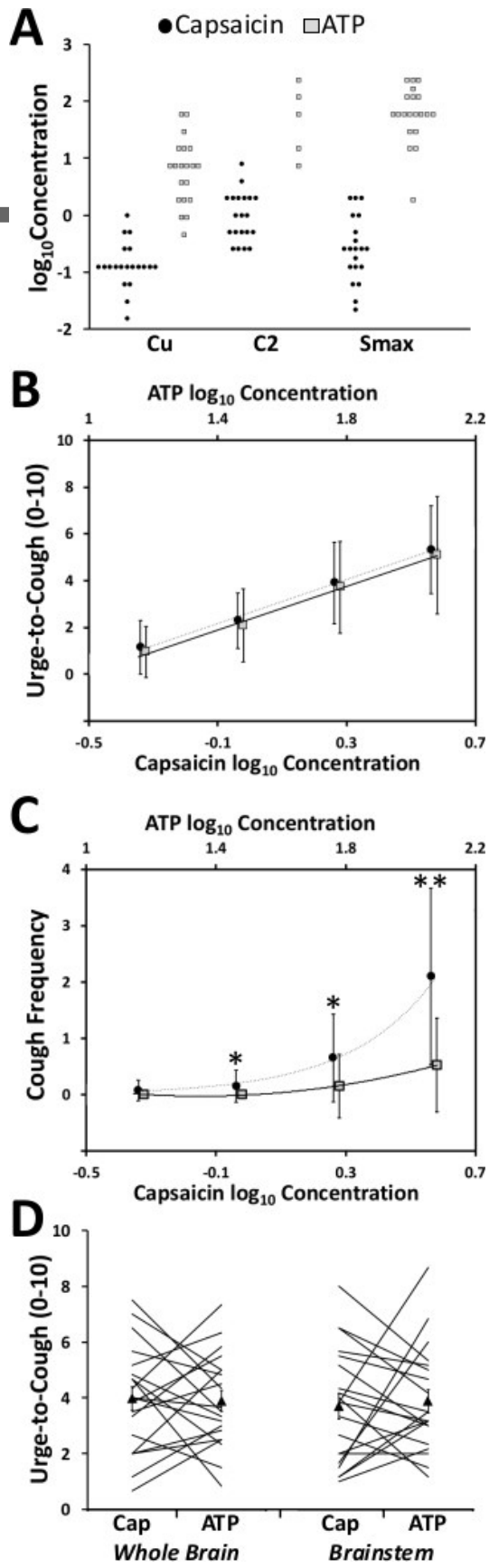


Figure 1.

A. Participants were challenged with single breaths of doubling concentrations of capsaicin and ATP to determine the lowest concentration to elicit a perceptible urge-to-cough (C_u) and two audible coughs (C_2). C_2 concentrations for ATP were obtained in five participants, but the remainder did not cough at any single inhalation of ATP up to the maximum administered concentration. Participants also inhaled the substances repeatedly for 24 seconds to determine the maximum concentration that could be inhaled while successfully suppressing cough (S_{max}). **B.** The stimulus-response relationships of the two tussive substances were assessed by recording urge-to-cough ratings after single breath inhalations of four successive concentration levels. **C.** Coughs were counted for 30 seconds after single breaths of four concentrations of the two substances and were significantly increased in frequency for capsaicin compared to ATP for concentrations of level 2 and greater. **D.** The mean levels of urge-to-cough during acquisition of functional brain images (represented by triangles) did not differ significantly between the two tussive stimuli. However, there was considerable variability in the relative levels of urge-to-cough across the participants, each of which is represented by a single line.

* $p < 0.05$ ** $p < 0.005$; Repeated measures ANOVA.

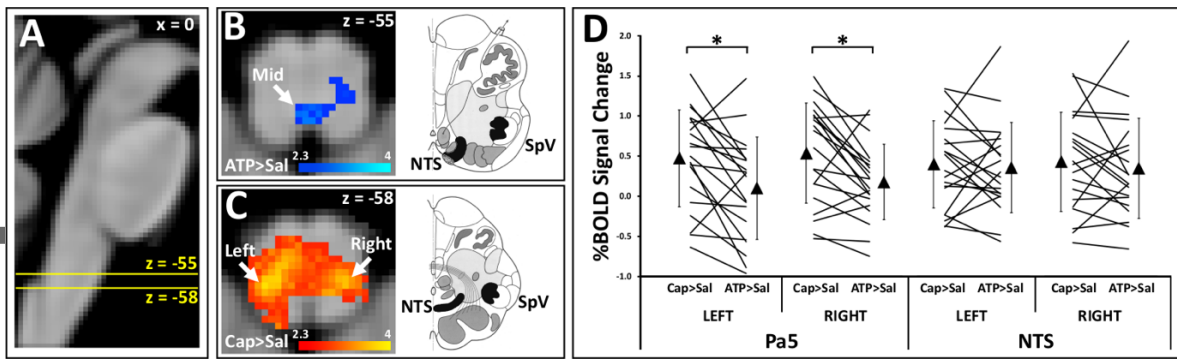


Figure 2.

A. A midline sagittal slice of the brainstem with yellow lines indicating caudal levels of the brainstem incorporating nuclei that respond to tussive stimulation. **B.** Activation for ATP>Saline (ATP>Sal) inhalation rendered in blue was observed in the dorsomedial medulla in a region likely to include the left and right NTS. The schematic indicates the locations of the NTS and spinal trigeminal nucleus (SpV) with black shading in the right hemi-section of the medulla at this level. **C.** Capsaicin>Saline (Cap>Sal) activation rendered in red-yellow extended symmetrically across the dorsal medulla with activation loci in lateral locations likely to include the Pa5, and a midline extent in the region including the NTS. The accompanying schematic indicates the likely locations of the NTS and SpV. **D.** BOLD signal changes for Cap>Sal and ATP>Sal were extracted from the left and right dorsal medullary regions, as well as the left and right sides of the midline region. Cap>Sal show significantly ($p=0.002$) increased BOLD signal compared to ATP>Sal in the left and right dorsal regions, whereas no difference between the stimuli was seen in the midline region; Repeated measures ANOVA.

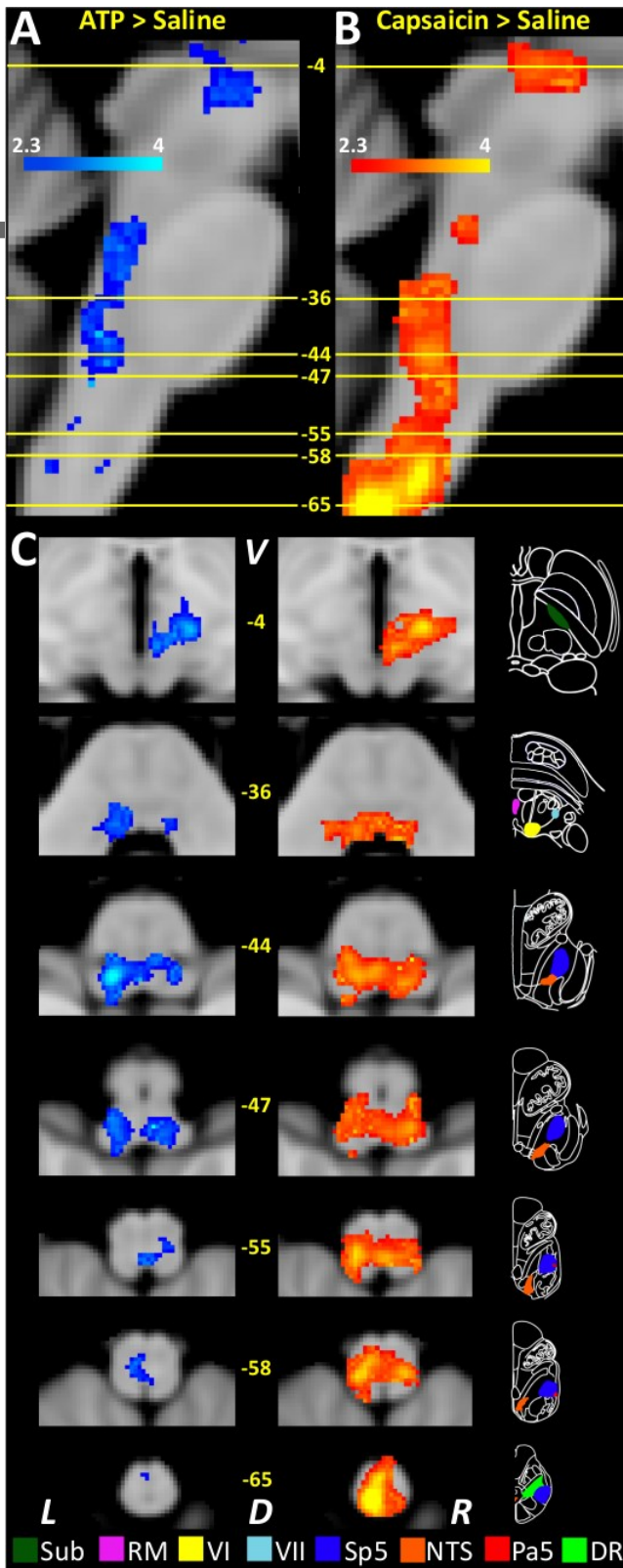


Figure 3.

A. A sagittal slice of the brainstem is rendered with ATP>Saline activation in blue. Yellow lines indicate the levels of axial slices shown in the lower panel of the figure. **B.** Capsaicin>Saline

activation is rendered in red-yellow on the midline sagittal slice of the brainstem. **C.** The panel shows a top-to-bottom series of progressively more caudal axial slices of the brainstem at levels below the anterior commissure in millimetres indicated by the yellow integers. Slices on the left show ATP>Saline activation (blue), and the slice on the right shows Capsaicin>Saline activation (red-yellow). A corresponding schematic of the brainstem accompanies each slice level, and includes selected nuclei in colour, the code for which is at the bottom of the panel. Activation to inhalation of both tussive stimuli was seen in the right midbrain ($z=-4$) in a cluster likely to incorporate the subthalamic nucleus (Sub). Bilateral dorsolateral mid pontine ($z=-36$) activations for both stimuli occurred in regions that could include the raphe magnus (RM) and the nuclei of the abducens (VI) and facial (VII) cranial nerves. More rostral levels of the medulla ($z=-44$ and $z=-47$) showed symmetrical dorsolateral ATP>saline and Capsaicin>Saline clusters of activations that likely incorporated both the nucleus of the solitary tract (NTS) and the spinal trigeminal nucleus (Sp5), including the paratrigeminal nucleus (Pa5). Sections at caudal levels of the medulla ($z=-55$ and $z=-58$) highlight discrepancies in the location of clusters for the respective tussive stimuli. Activation extending laterally to include the Sp5 and Pa5 is seen for Capsaicin>Saline, but not for ATP>Saline. The most rostral level of the medulla ($z=-65$) shows Capsaicin>Saline activation likely to incorporate the dorsal reticular nucleus, that is not seen for ATP>Saline activation. [Note – Axial slices are ventral at top, and left side on left of image.]

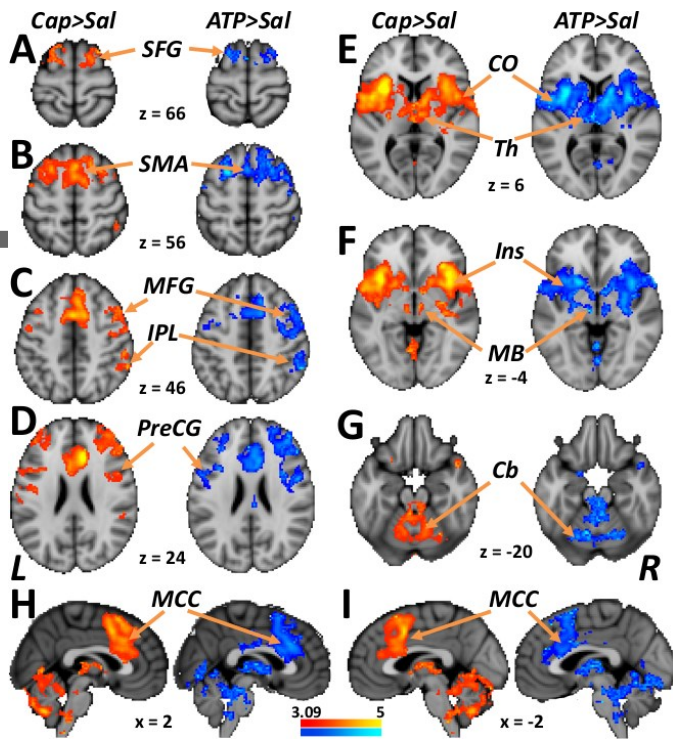


Figure 4.

A. Regional activations for Capsaicin>Saline (Cap>Sal) are rendered in red-yellow, and for ATP>Saline (ATP>Sal) activations are rendered in blue on axial slices of a standard brain. Symmetrical activation in the premotor cortex of the superior frontal gyrus (SFG) was seen for inhalation of both tussive stimuli. **B.** The supplementary motor area (SMA) activated in response to both capsaicin and ATP. **C.** Activation for both capsaicin and ATP in the middle frontal gyrus (MFG) and inferior parietal lobule (IPL) was seen in the right hemisphere. **D.** Bilateral activation for both tussive stimuli occurred in the precentral gyrus (PreCG). **E.** The central operculum (CO) and the thalamus (Th) showed symmetrical activation in response to capsaicin and ATP. **F.** Activation in responses to both tussive stimuli was seen extensively throughout the insula (Ins) in both hemispheres. Midbrain (MB) activations to the two stimuli were also seen bilaterally. **G.** The cerebellum (Cb) activated in the vermis and lobes of the cerebellum in response to capsaicin and ATP. **H.** Capsaicin and ATP activation was seen in the mid cingulate cortex (MCC) in the right hemisphere, **I.** and in the left hemisphere.

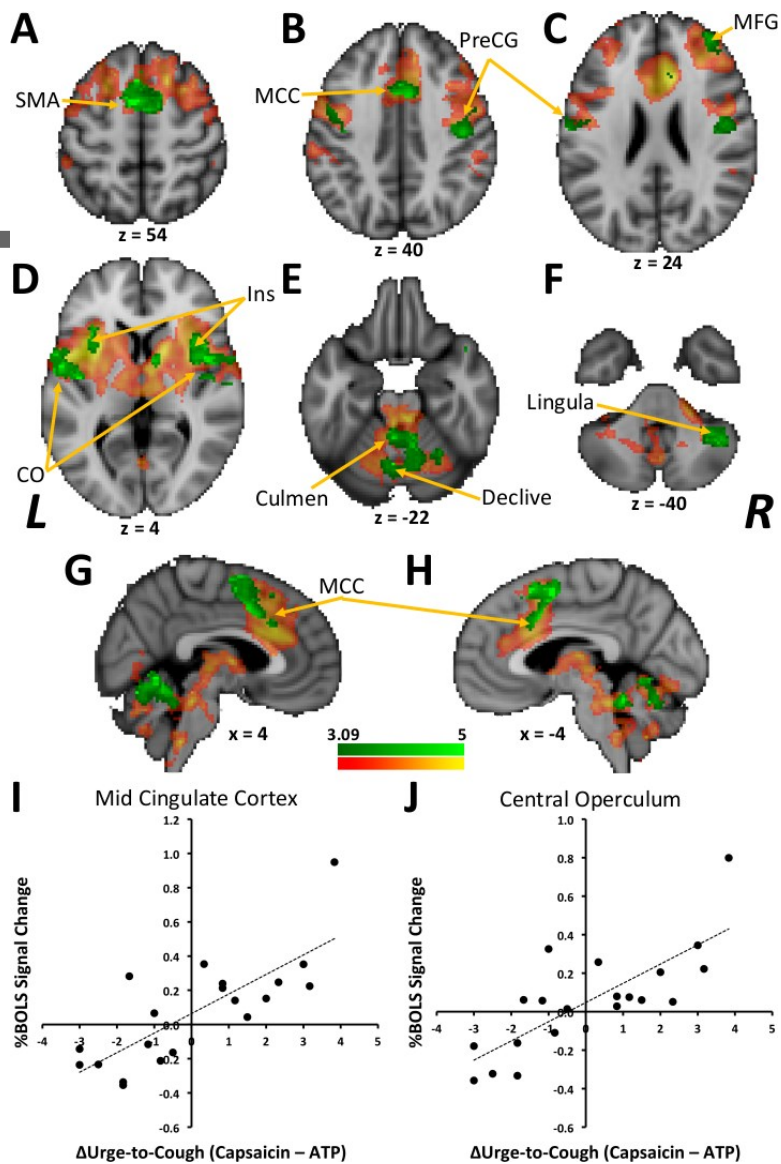


Figure 5.

A. Regions distributed throughout the brain with responses to ATP and capsaicin are rendered in red-yellow in the images in this figure. The image contrast of Capsaicin>ATP was tested for associations with behaviour using a difference score of urge-to-cough ratings during whole brain scanning (Capsaicin minus ATP). Regions showing an association between stimulus-related differences in activation levels and intensities of urge-to-cough are rendered in green, and were seen in the supplementary motor area (SMA) at z=54. **B.** The mid cingulate cortex (MCC) and the precentral gyrus in both hemispheres showed activation levels associated with urge-to-cough rating differences. **C.** The middle frontal gyrus in the right hemisphere showed rating difference-related variance in the contrast of Capsaicin and ATP activation. **D.** Bilateral regions of the central operculum (CO) and insula (Ins) showed an association between difference scores and activation levels. **E.** Shared variance between rating differences and activation levels were seen in the cerebellum in the

culmen, declive, **F.** and lingula. **G.** Activation levels in the mid cingulate cortex (MCC) correlated (Pearson's test) with differences in urge-to-cough ratings in the right hemisphere, **H.** and the left hemisphere. **I.** Examples of the relationship between urge-to-cough and activation levels are shown in the scattergrams. Participants with increased urge-to-cough levels during capsaicin inhalation compared to inhalation of ATP showed the highest levels of relative BOLD signal change differences for the contrast of the two activations (Capsaicin>ATP) in the mid cingulate cortex. This pattern was reflected symmetrically, whereby increasing levels of the inverse comparison, represented by relatively negative values, tended to decrease to similar degrees. **J.** A second scattergram using data from the central operculum further illustrates the relationship between activation levels and behavioural ratings.

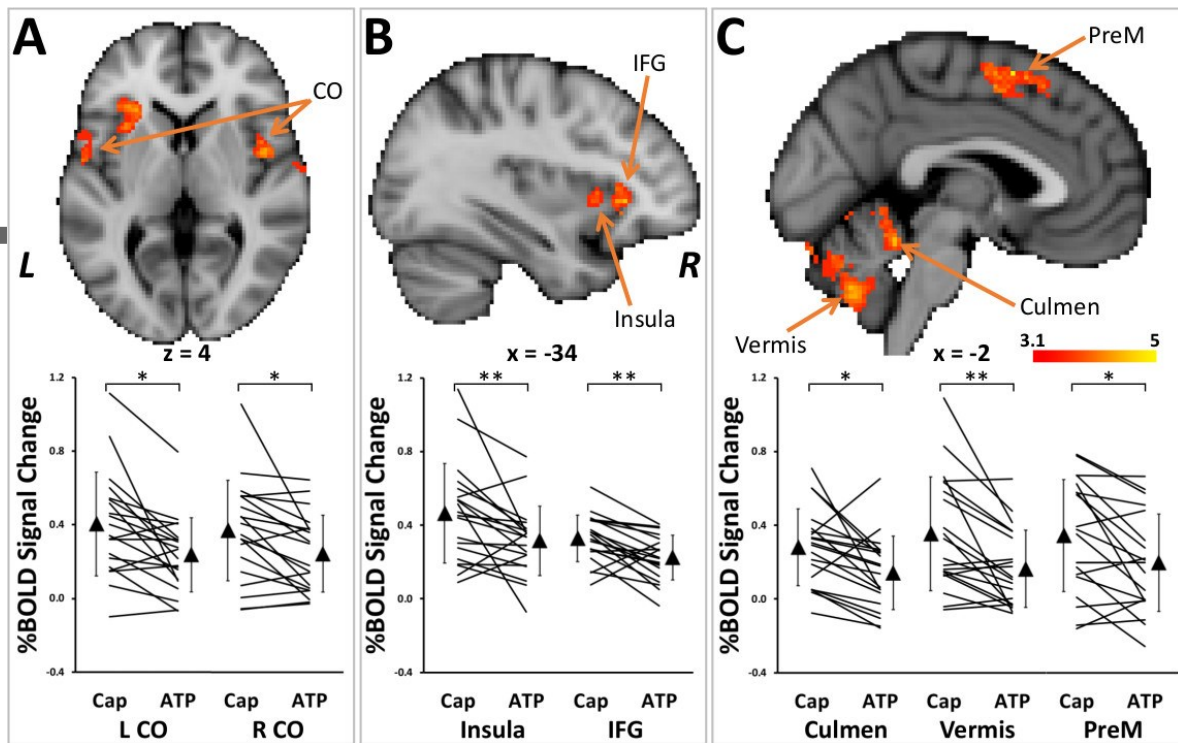


Figure 6.

A. The contrast of Capsaicin>ATP is rendered on a standard brain in red-yellow. An increased level of capsaicin activation that was greater than ATP activation was seen in the central operculum (CO) in both hemispheres. The column graph in the panel shows the average capsaicin and ATP-related BOLD signal changes from the left (L) and right (R) central operculum (error bars are SEM). BOLD signal changes during capsaicin inhalation were significantly increased compared to ATP inhalation in both of the regions of interest. **B.** The cerebellum showed significantly increased levels of BOLD signal change during capsaicin compared to ATP inhalation in the culmen, **C.** and the vermis. **D.** The inferior frontal gyrus (IFG) and the anterior insula had increased capsaicin inhalation BOLD signal changes that were greater than responses to ATP. **E.** Bilateral midline premotor cortices had increased capsaicin-related BOLD signal changes compared to ATP and is shown in the left hemisphere in this panel. * $p < 0.01$ ** $p < 0.001$; Paired t-tests.

Table 1. Regions in brain hemispheres showing activation during inhalation of tussive substances.

REGION	Capsaicin>Saline				ATP>Saline			
	<i>Peak coordinate</i>				<i>Peak coordinate</i>			
	<i>x</i>	<i>y</i>	<i>z</i>	<i>Z score</i>	<i>x</i>	<i>y</i>	<i>z</i>	<i>Z score</i>
Superior Frontal Gyrus	28	14	60	4.56	-2	8	62	5.76
	2	22	50	6.66	26	12	58	4.52
	-24	14	60	5.43	-20	10	58	5.32
SMA	-4	2	58	4.62				
Middle Frontal Gyrus	48	16	46	4.01	44	8	52	4.51
	-42	12	50	3.96	48	16	42	4.68
	48	36	28	4.65	50	30	24	5.30
	-38	46	26	4.93	-38	40	26	6.02
Inferior Parietal Lobule	56	-38	48	3.95	56	-36	48	4.96
Precentral Gyrus	44	-12	42	4.41	42	-14	36	4.60
	-46	-12	42	5.29	-50	-6	40	5.74
Central Operculum	46	6	6	4.34	44	2	2	4.92
	-46	6	6	7.28	-50	4	4	4.81
Mid Cingulate Cortex	10	6	40	5.26	12	10	46	4.25
	-4	8	42	5.84	-4	6	42	5.27
	6	22	22	6.36	12	20	36	4.80
	-4	12	24	5.56	-2	10	32	6.03
Insula	38	18	-2	5.33	36	8	0	4.73
	-32	12	4	8.02	-30	10	4	5.40
Putamen	28	10	-4	6.07	24	4	-6	4.39
	-22	12	-8	5.59	-20	10	-4	4.86

Thalamus	12	-12	10	7.24	12	-14	12	5.13
	-16	-16	2	4.01	-8	-16	4	5.62
Midbrain	4	-22	-2	4.52	10	-18	-6	4.29
	-8	-20	-2	4.45	-8	-20	-4	4.95
Cerebellum	16	-58	-16	5.45	6	-46	-16	4.53
	-6	-64	-16	4.57	30	-62	-28	4.85
	8	-46	-22	4.81	-22	-64	-22	4.83
	-6	-44	-20	4.91				
	0	-64	-42	4.60				

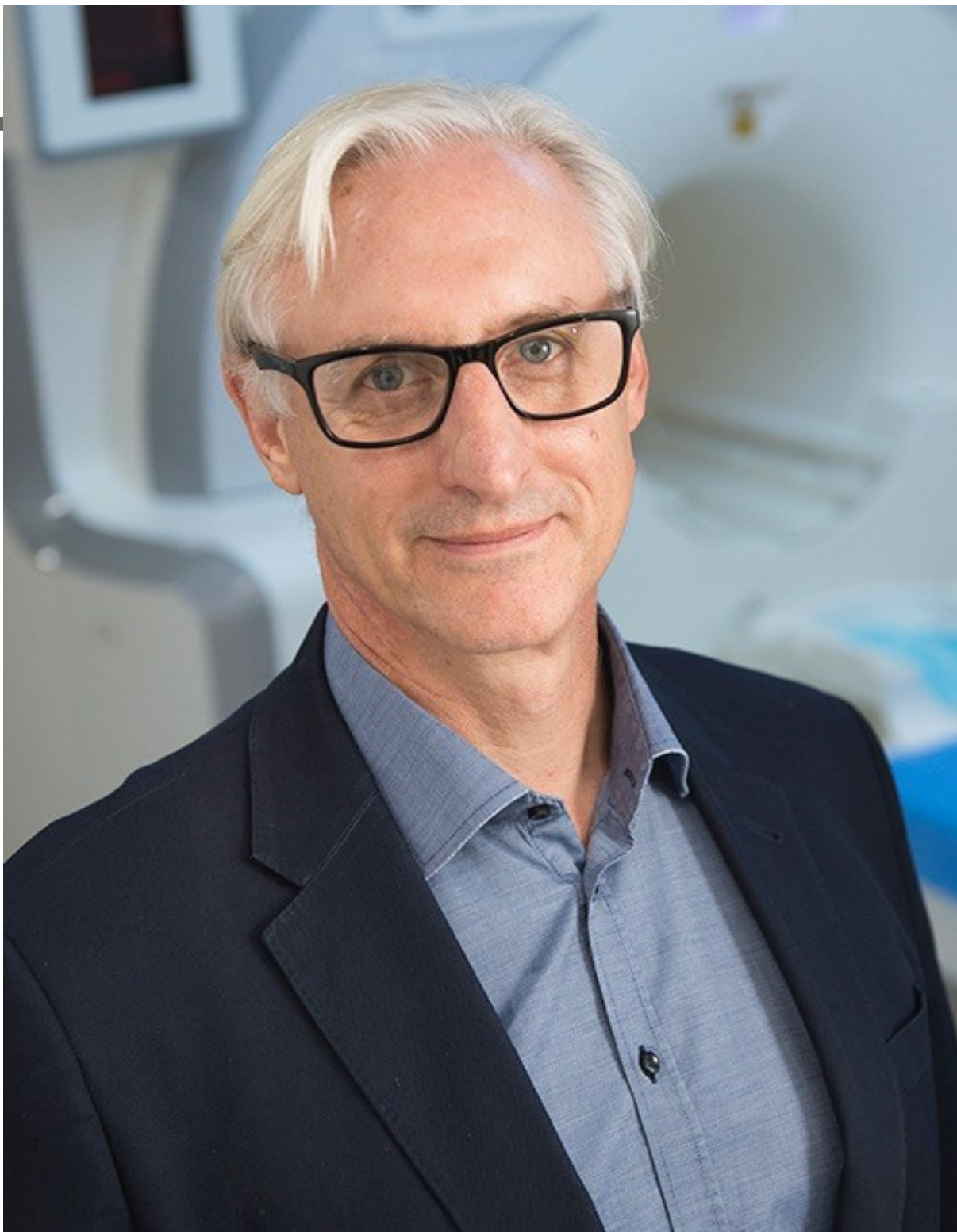
Table 2. Regions in brain hemispheres where levels of Capsaicin>ATP contrast were correlated with difference in urge-to-cough ratings between the two tussive substances.

REGION	Urge-to-Cough Correlates			
	<i>Peak coordinate</i>			
	<i>x</i>	<i>y</i>	<i>z</i>	<i>Z score</i>
Supplementary Motor Area	-2	4	52	5.71
Superior Frontal Gyrus	-2	-18	54	6.03
Precentral Gyrus	38	-16	42	4.52
	-38	-16	40	3.95
Middle Frontal Gyrus	34	52	22	4.82
Primary Sensorimotor Cortex (BA43)	-56	-2	14	6.35
Central Operculum	44	4	4	5.17
	-48	-8	6	5.43
Insula	36	18	2	4.42
	-34	18	2	4.74
Cerebellum	-4	-46	-20	5.36
	-4	-64	-22	5.46
	44	-54	-42	4.54

Table 3 Regions in the brain hemispheres where activation levels during capsaicin inhalation were increased compared to responses to ATP inhalation.

REGION	Capsaicin>ATP			
	<i>Peak coordinate</i>			<i>Z score</i>
	<i>x</i>	<i>y</i>	<i>z</i>	
Medial Frontal Gyrus	-2	8	58	3.90
Central Operculum	62	10	2	4.13
	-54	6	2	3.53
Inferior Frontal Gyrus	-34	28	0	3.58
Insula	-30	24	6	3.57
Cerebellum	-2	-46	-20	3.52
	-2	-66	-40	3.52

Author Manuscript



This article is protected by copyright. All rights reserved.